ULTRASONIC STUDIES OF COMPOSITES UNDERGOING THERMAL AND FATIGUE LOADING

Eric I. Madaras, William P. Winfree, Patrick H. Johnston
NASA Langley Research Center
MS 231
Hampton, VA 23681-0001

INTRODUCTION

New composite materials possess attractive properties for use in advanced aircraft. A necessary requirement for their introduction into aeronautic use is an accurate understanding of their long term aging processes so that proper design criteria can be established. In order to understand those properties, these composites must be exposed to thermal and load cycles that are characteristic of flight conditions. Additionally, airline companies will require nondestructive evaluation (NDE) methods that can be used in the field to assess the condition of these new materials as they age.

As part of an effort to obtain the required information about new composites for aviation use, we are performing ultrasonic measurements both in the NDE laboratory and in the materials testing laboratory at NASA. The materials testing laboratory is equipped with environmental chambers mounted on load frames so that composite samples can be exposed to thermal and loading cycles representative of flight protocols. Applying both temperature and load simultaneously will help to highlight temperature and load interactions during the aging of these composite materials.

This study reports on our initial ultrasonic attenuation results from thermoset and thermoplastic composite samples. Ultrasonic attenuation measurements have been used reliably to assess the effects of material degradation. For example, recently, researchers have shown that by using frequencies of ultrasound on the order of 24 MHz, they could obtain adequate contrast in the evaluation of thermal degradation in these composites. [1] This paper will present data that shows results at a lower frequency range. In addition, we report results on the frequency dependence of attenuation as the slope of attenuation with respect to frequency, $\beta = \Delta\alpha(f)/\Delta f$. The slope of attenuation is an attractive parameter since it is quantitative, yet does not require interface corrections like conventional quantitative attenuation measurements. This is a consequence of the assumption that

interface correction terms are frequency independent. Uncertainty in those corrections terms compromises the value of conventional quantitative attenuation data. [2, 3].

EXPERIMENT

The samples are 16 and 32 ply thick dog bone shaped panels manufactured by major aeronautic companies. Each sample is 122 cm long by 30.5 cm wide. The thermoset composites consist of IM7 fibers embedded in a 5260 matrix and the thermoplastic composites consist of IM7 fibers embedded in K3B matrix.

Figure 1 illustrates one example of the flight load and temperature profile to which these composite samples are exposed. The flight load is expressed in terms of microstrain. Strain and temperature curves represent runway loads, climbing and descending loads and cruising loads. The low strain profile peaks near 2000 μstrain. The high strain profile peaks near 3000 μstrain. The temperature profile for the samples reported here reaches a peak temperature of 280^{o} F.

The measurements are made with two separate ultrasonic pulse echo systems. They use a 5 MHz, 5 cm focal length, 1.2 cm diameter submersion transducer. The ultrasonic systems are microcomputer controlled to synchronize the measurements with x-y positions. The NDE laboratory C-scan system consists of a water tank, and uses a conventional pulser-receiver and a 100 MHz 8 bit digitizing oscilloscope to record the data. It was preferred that the aging protocol would not be disrupted by removing the samples

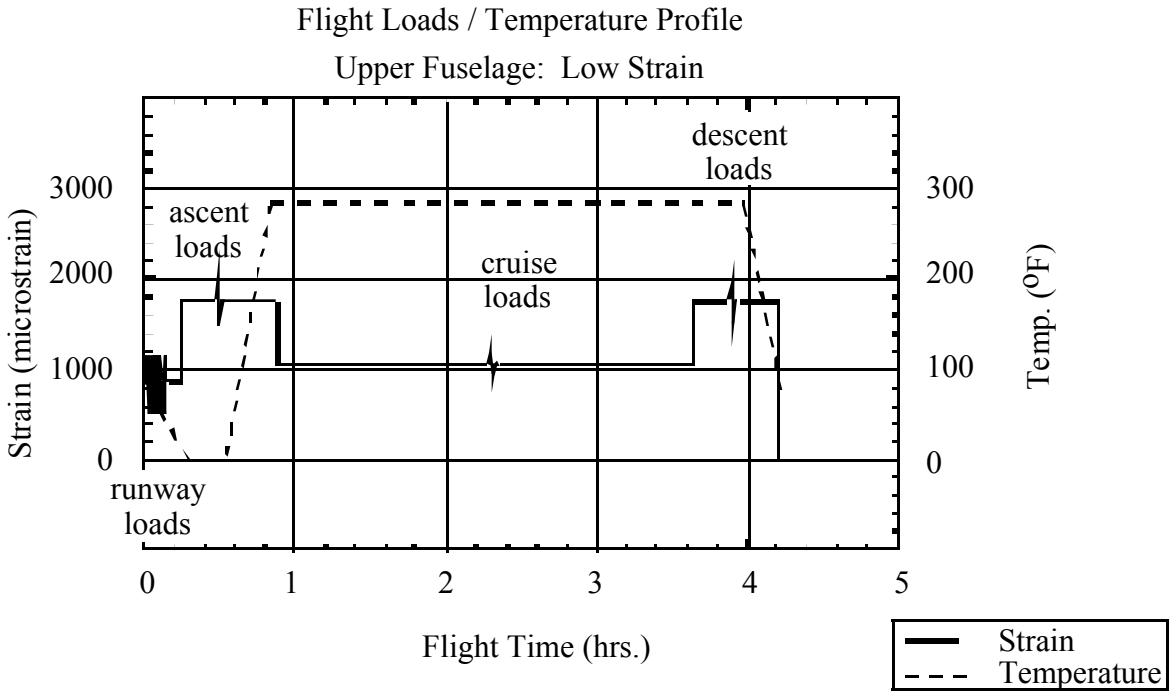

Figure 1. Representative flight strain loads and thermal loads that are used to study the aging process in composites. The strain levels are indicated on the left axis and shown as a solid line. The temperature levels are indicated on the right axis and shown as a dashed line. The horizontal axis shows the flight time in hours.

from the environmental chambers frequently, so a second in-situ scanning system was constructed to measure the composite samples while they are mounted in the environmental chambers. This in-situ system constrained the scan regions to those areas of the composite samples that are exposed inside the chambers, but allowed more frequent measurements. The in-situ system uses a broad band pulser-receiver computer card along with a 100 MHz 8 bit digitizing card mounted in the microprocessor. For this study, this system digitized at 25 MHz. The samples were scanned in raster format in 0.254 cm steps. In the environmental chamber scanning system, the images from adjacent scanned regions are tiled together to produce a composite image.

The ultrasonic measurements in the water tank use a "shadowed glass" method. In that method, the echo amplitude from a glass reflector without the composite present is used to normalized the echo amplitude from the glass reflector with the composite attenuating the beam. This measure of attenuation is then corrected for transmission losses and normalized for thickness. Eq. 1 expresses the attenuation as

$$\alpha = \ln[(A_2/A_1)*T_{wc}^{\,2}]/2t \qquad (1)$$

where α is the attenuation in Np/cm, A_2 is the glass reflector echo signal magnitude with the composite in place, A_1 is the glass reflector echo signal magnitude without the composite in place, T_{wc} is the product of the two transmission coefficients that represent sound passing from water into the composite and then from the composite into water, and t is the thickness.

The ultrasonic system that measures the composites in the environmental chambers differs from the water tank in that the ultrasound is coupled into the sample through water but there is only air on the back of the composite. To estimate the material attenuation in the composite for this case, we use the sample's front and back wall ultrasonic echoes at each measurement site. We calculate the slope of attenuation with respect to frequency from our measurements by first calculating the Fast Fourier Transform (FFT) power spectrum for two adjacent interface echoes. We then use the first echo's FFT power spectrum, $S_k(f)$, to normalize the subsequent echo's FFT power spectrum, $S_{k+1}(f)$, frequency by frequency. Finally, we convert the data to logarithmic form and normalize by thickness to obtain an apparent attenuation, $\alpha_a(f)$, which is not corrected for interface losses:

$$\alpha_a(f) = \ln [S_{k+1}(f) / S_k(f)] / 2t. \qquad (2a)$$

This data was then fitted to a linear equation:

$$\alpha_a(f) = \beta * f + C\ , \qquad (2b)$$

where β is the slope of the data and C is the function's intercept. Since the interface transmission and reflection coefficients are assumed to be frequency independent, they will in general be reflected in the intercept term, C, while β will represent the frequency dependent components of the materials. In figure 2a we depict the power spectrum as a

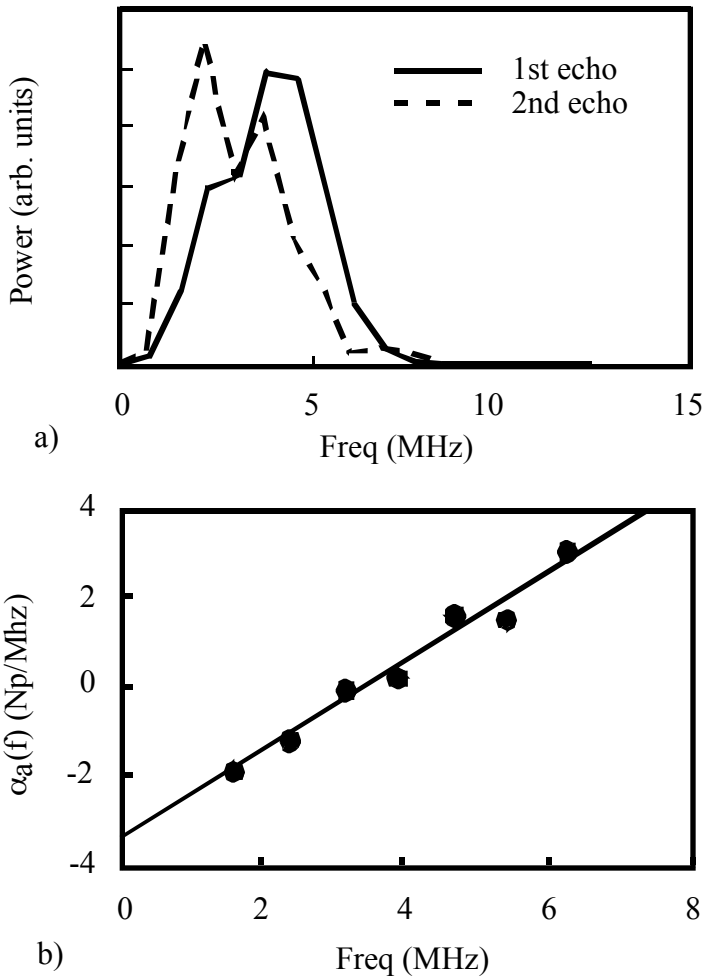

Figure 2. The top figure shows the power spectrum as a function of frequency for two adjacent ultrasonic echoes. The lower figure shows the frequency dependent apparent attenuation, $\alpha_a(f)$, as a function of frequency and the straight line fit to the data.

function of frequency from two adjacent echoes at one site. Figure 2b shows the function $\alpha_a(f)$ as a function of frequency and illustrates the near linear behavior of the data. We process the data in this manner at each independent site.

RESULTS AND DISCUSSION

The first samples that we discuss are the IM7/5260 thermoset matrix samples. Figure 3 illustrates several panels at several ages. These panels underwent the high strain load/thermal protocol. Figures 3a and 3b show the virgin materials before any aging has begun. Figure 3c represents a panel that was measured at 5,000 hours and figure 3d shows a panel that was measured after 10,000 hours of thermal/load cycling. The panels at zero hours show the lowest attenuation with relatively large attenuation variations as seen by the texture in figs. 3a and 3b. At 5,000 hours, the attenuation has increased while the texture variations have moderated. There is a modest attenuation increase at the free edges of that sample (top and bottom of figure 3c). At 10,000 hours the attenuation has continued to increase with a nearly 45% increase on average. In this sample there is a strong attenuation increase at the edges of the sample that indicate damage ingression from the edges which increases the variance in the measurement.

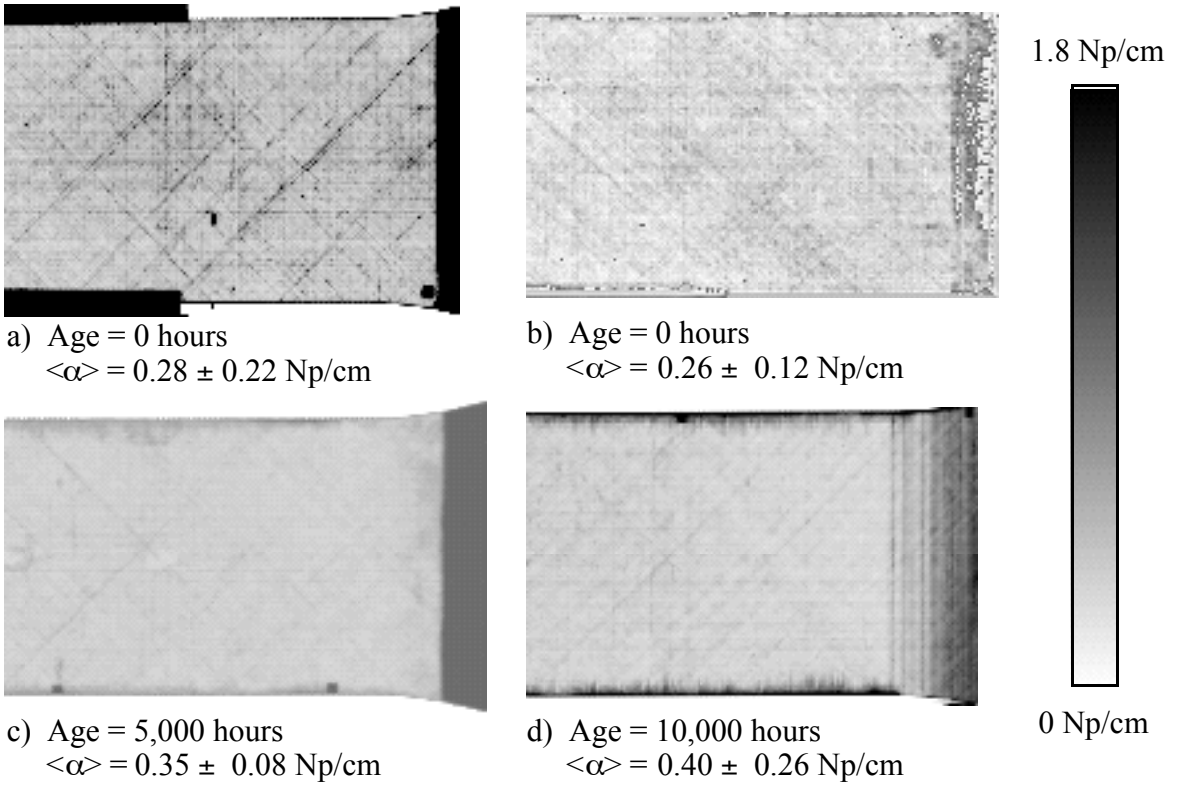

a) Age = 0 hours
<α> = 0.28 ± 0.22 Np/cm

b) Age = 0 hours
<α> = 0.26 ± 0.12 Np/cm

c) Age = 5,000 hours
<α> = 0.35 ± 0.08 Np/cm

d) Age = 10,000 hours
<α> = 0.40 ± 0.26 Np/cm

Figure 3. Ultrasonic attenuation images panels of IM7/5260, 32 ply, at different ages subjected to the high strain protocol. Each figure shows the detail for half a panel and the age, average attenuation, <α>, and standard deviation are listed below each figure. The figures are scaled from 0 (white) to 1.8 Np/cm (black).

Closer inspection of the details of the edge structure from figure 3d is shown in figure 4. Fig. 4a. shows an enlargement of the edge. The rf data is shown in Fig. 4b and 4c. Fig. 4b shows a front wall echo, several back wall echoes and the glass reflector echo. Fig. 4c shows the same sequence, but now the echoes from between the front and back wall echoes are larger with a strong echo developing midway between the front and back. Comparing the signals seen in Fig. 4b and 4c illustrate that delamination-like damage is forming at the edges. This would increase the attenuation at the edges as seen.

The degradation behavior of the thermoplastic composite, IM7/K3B panels, presents itself in a different manner. As can be seen in figure 5a compared with 5b, the IM7/K3B 16 ply panel which was subject to the high strain load/thermal protocol shows a very large increase in attenuation (~400%) after only 5,000 hours. Also, very noticeable are the many small islands of high attenuation. They appear to have an orientation that is predominately perpendicular to the loading direction, and suggests preferential local damage along the 90^{o} direction. Similar degradation was seen for the low strain loading/thermal protocol. That data indicated a 50% increase in attenuation after only 3,000 hours. Figure 6 shows the raw rf data from two areas indicated in fig 5b. Fig 6a shows the raw data a general background attenuation region while 6b shows data from a region which contains high attenuation.

In figure 7, we show a comparison of the slope of attenuation results from measurements made in the environmental chambers. The small localized areas of higher

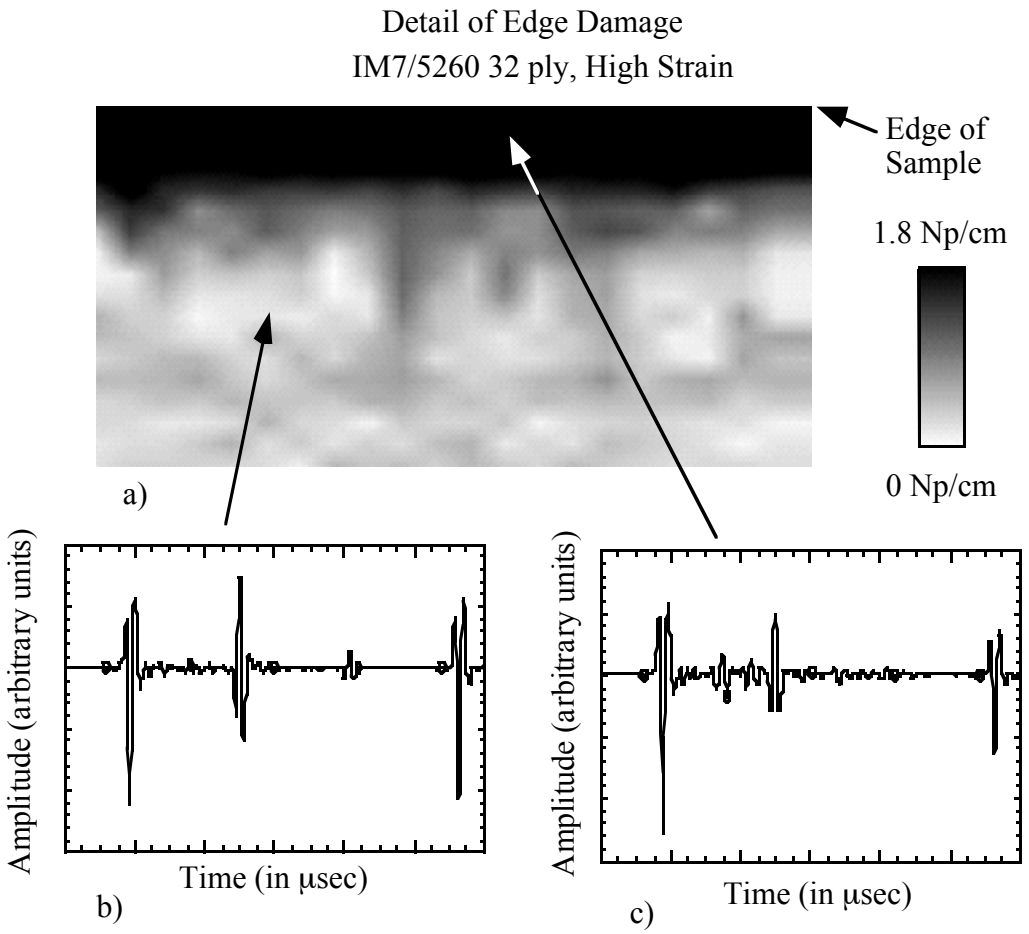

Fig. 4. Ultrasonic details of the damage visible at the edge of sample shown in Fig. 3d. Panel a is a close-up detail of the edge. Panel b is an rf amplitude plot versus time from an undamaged region for comparison with panel c which is an rf amplitude plot versus time from a damaged region. Fig. 4a is scaled in the same manner as Fig. 3.

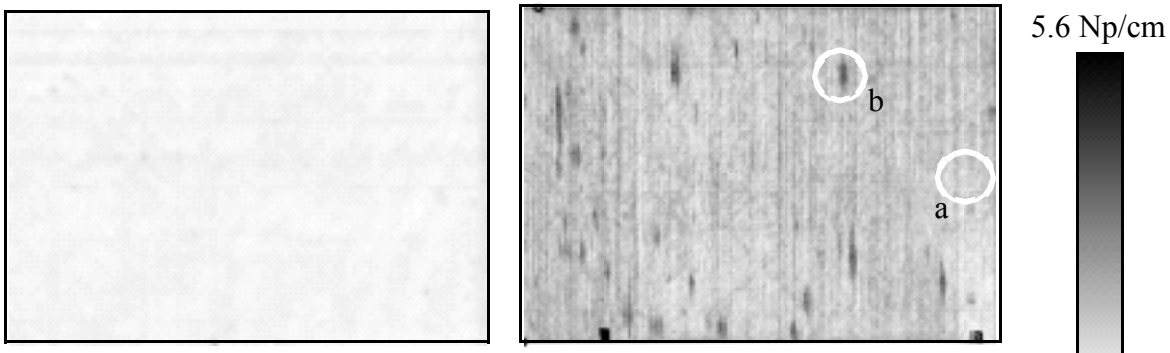

Fig. 5 Ultrasonic images of a IM7/K3B, 16 ply panel undergoing high strain and thermal aging. Each figure shows the detail for half a panel and the age, average attenuation, $\langle\alpha\rangle$, and standard deviation are listed below each figure. The circled areas are addressed in figure 6. The figures are scaled from 0 (white) to 5.6 Np/cm (black).

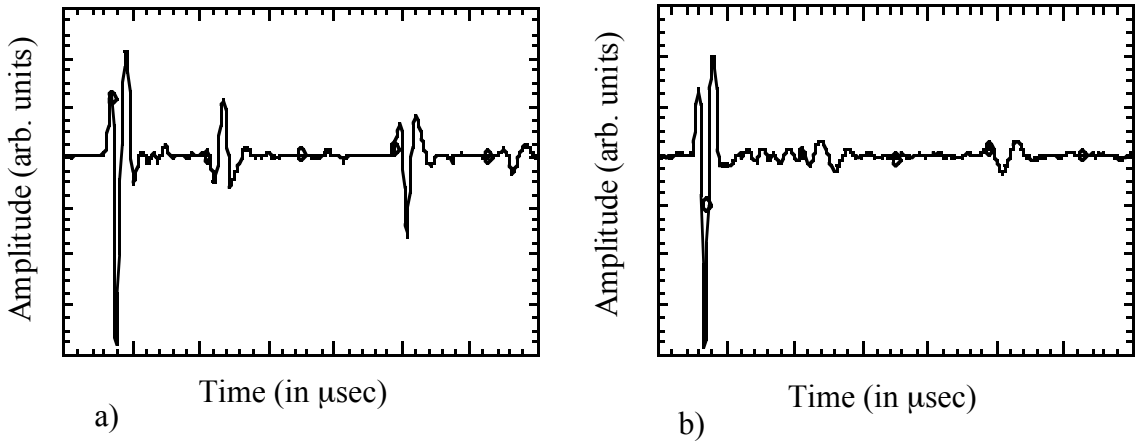

Fig. 6 Details of localized damage in an IM7/K3B, 16 ply panel which has undergone a high strain load/thermal exposure protocol. Panel a shows the ultrasonic signal from a general region representative of the region labeled as "a" in figure 5b, while the signal in panel b shows the significant signal losses in the center of the localized area representative of the region labeled as region "b" in figure 5b.

attenuation are visible in both figures 7a and 7b, and are similar to those seen in Figs. 5b. The slope of attenuation shows a large increase when comparing the 3,000 and 7,000 hours data.

Figure 8 compares the average slope of attenuation data taken from two groups of panels in the environmental chambers as a function of aging for the IM7/K3B materials. If we group the data according to the strain levels that they were exposed to, we can see an approximately linear relationship between the slope of attenuation and the composite's age. The 50% increase in strain resulted in a nearly four fold increase in the rate of increase in the slope of attenuation behavior with aging from this data.

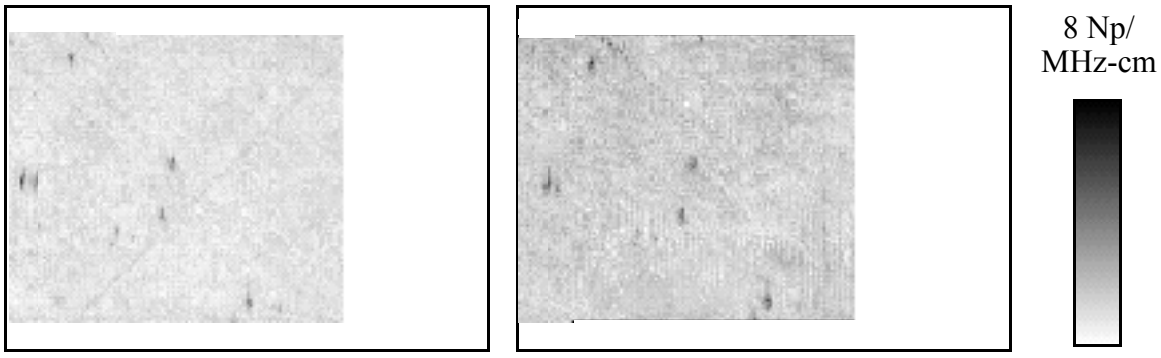

Fig. 7 Ultrasonic slope of attenuation, β, images of an IM7/K3B, 16 ply panel which has undergone a low strain load/thermal protocol. Each figure shows the scanned region for half a panel and the age, average slope of attenuation, <β>, and standard deviation are listed below each figure. The figures are scaled from 0 (white) to 8 Np/MHz-cm (black).

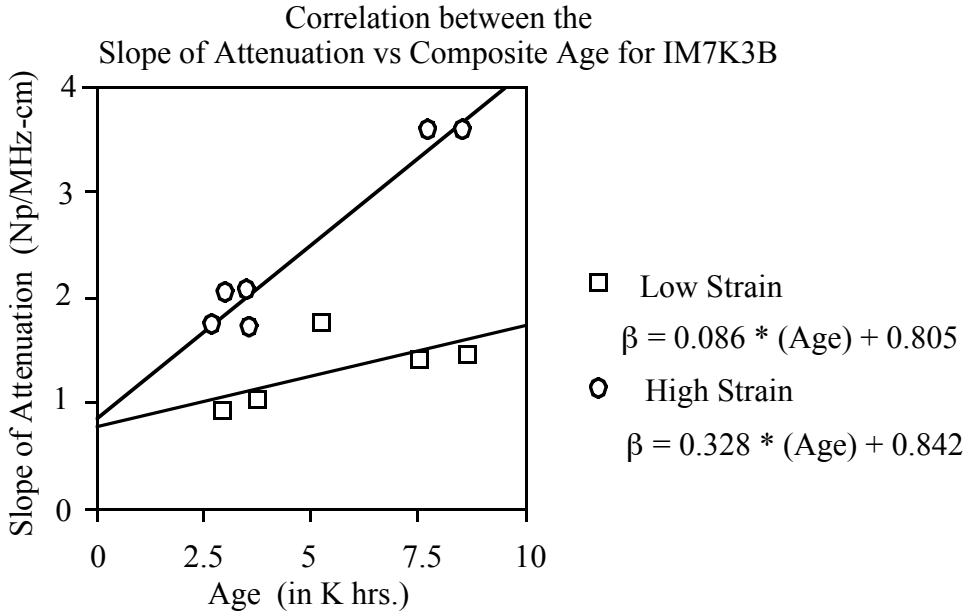

Figure 8. Correlation between slope of attenuation vs. composite age for IM7/K3B composites. The open squares represent data taken with the low strain levels. The open circles represent data taken with the high strain levels.

CONCLUSION

We measured the ultrasonic attenuation of IM7/5260 and IM7/K3B panels that are undergoing load and thermal cycling for long term aging studies. These measurements were made with an in situ system in the materials testing laboratory as well as with a conventional water tank based system in the NDE laboratory. Both the IM7/5260 and IM7/K3B panels show large increases in ultrasonic attenuation over 5,000 to 10,000 hours of aging. In the case of the IM7/5260 panels, primary damage occurred at the panel's edges as early as 5,000 hours, and grew inward. The IM7/K3B panels behaved differently because they showed a significant global increase in ultrasonic attenuation with widely distributed localized damage sites. Finally, the data from a small number of samples suggests that the slope of attenuation parameter, β, demonstrates a good correlation with aging and the two loading protocols when applied to the IM7/K3B composite panels.

In the future, as these panels reach their age goals, they will be destructively tested to obtain the resulting material parameters. This data will be compared with the NDE data. In addition, we plan in situ measurements of stiffness coefficients with Lamb waves.

REFERENCES

1. D. J. Chinn, P. F. Durbin, G. H Thomas, and S. E. Groves, in *Review of Progress in QNDE*, vol. 16, Eds. D. O. Thompson and D. E. Chimenti (Plenum, New York, 1997), p. 1893.
2. S.M. Handley, M.S. Hughes, J.G. Miller, and E.I. Madaras, *Proc. IEEE Ultrasonics Symposium* (Denver, 1987), 87CH2492-7, pp. 827-830, 1988.
3. David K. Hsu and Ali Minachi, *Review of Progress in QNDE*, Vol. 9B, Eds. D.O. Thompson and D.E. Chimenti, (Plenum, New York, 1990), pp. 1481-1488